Electronic Supplementary Information for

Photocarrier Dynamics in Perovskite-based Solar Cells Revealed by Intensity-Modulated Photovoltage Spectroscopy

Xiaoqing Chen[*]*, Yasuhiro Shirai, Masatoshi Yanagida and Kenjiro Miyano*[*]

The IMVS technique is often regarded as a complementary method to transient photovoltage (TPV), [1–5] which is another small perturbation method widely used in PSCs.[6–9] Recall that the two methods are not independent because the TPV result in time domain and the IMVS signal in the frequency domain are connected through Fourier transformation. Their equivalence is confirmed as shown by Fig. S1, in which the IMVS signal is compared with the Fourier transform of TPV result taken under the identical illumination conditions. Since these two methods are mathematically equivalent, the published results from both methods are quoted in this article without distinction.

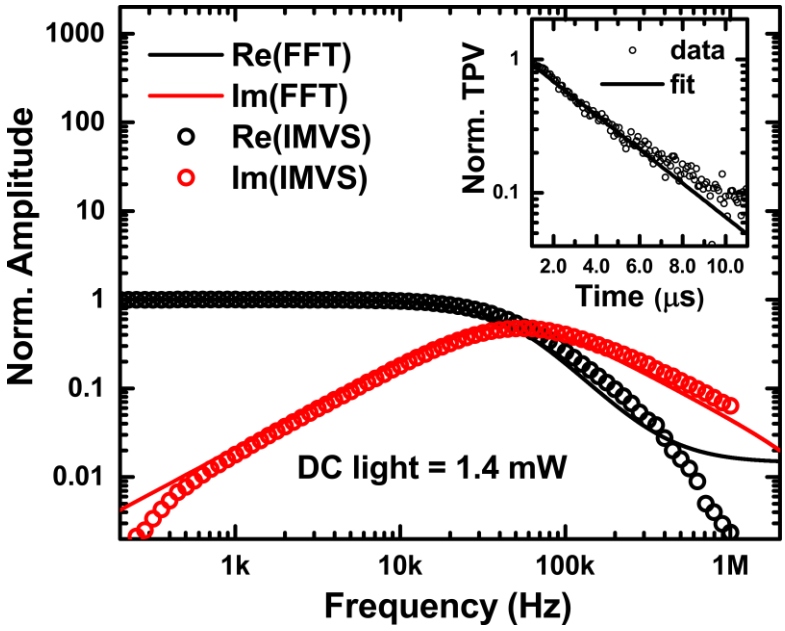

Fig. S1. Comparison between the normalized IMVS signal and the normalized amplitude-frequency profile of TPV calculated from fast Fourier transform. Both results are obtained at DC light P_0 = 1.4 mW. The inset shows the normalized TPV curve in time domain.

Device Characterization

In the IMVS experiment, the perovskite solar cell is excited with a 638 nm-laser diode (Thorlabs L638P700M) driven by a Thorlabs LTC100-A control set and modulated by a Solartron 1255B frequency response analyzer. The modulation depth is <10% of the DC light intensity. The total light intensity is tuned with a variable neutral density filter. Meanwhile the photovoltage response is recorded with the above mentioned Solartron frequency analyzer. On the widely used Cole-Cole plot, any recombination process corresponds to a semi arc. For example, in our experiment, when the device is illuminated by low excitation power (35 nW), there is one arc corresponding to 10 Hz (16 ms) (Fig. S2b); while under high excitation power (1 mW), there are two arcs corresponding to 14 Hz (11 ms) and 37 kHz (4.3 μs) (Fig. S2c), respectively.

In the temperature dependence measurement, the sample temperature is controlled by an Etac Hiflex Keyless Chamber. The IV curves are measured with a commercial system (SYSTEMHOUSE SUNRISE corp., Japan).

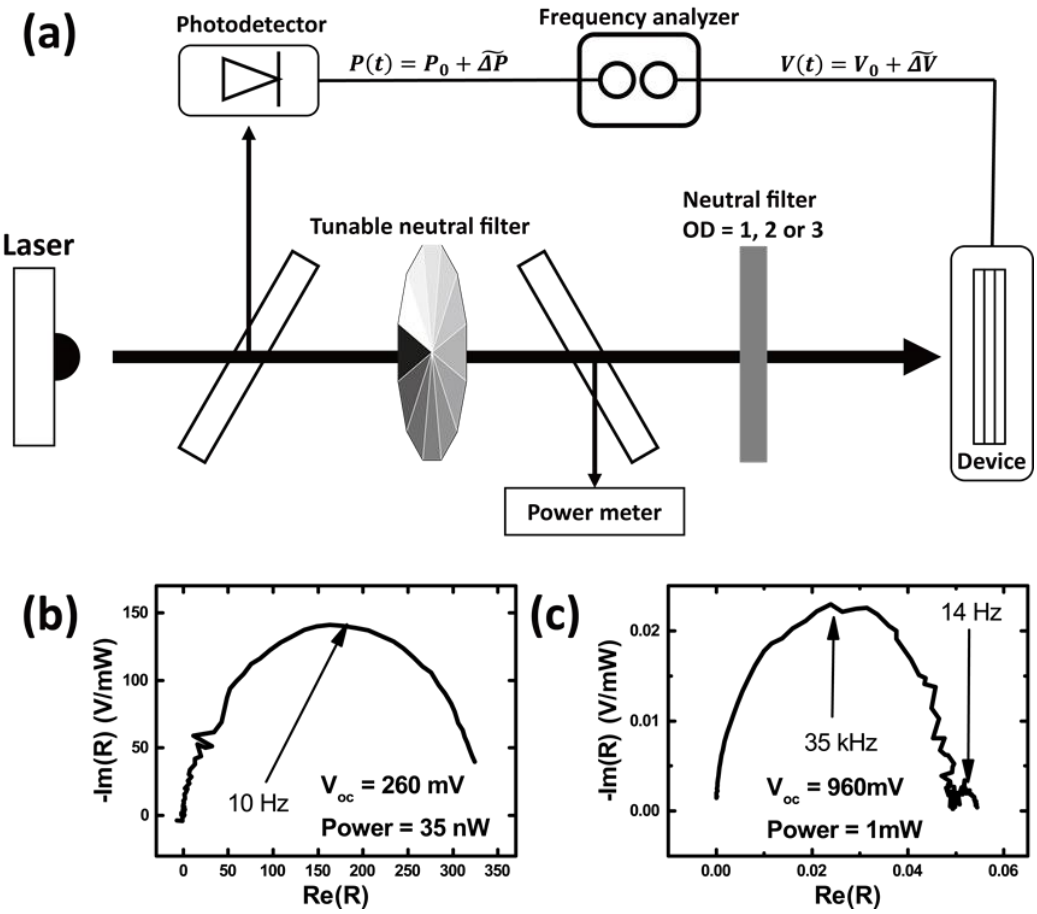

Fig. S2. (a) Scheme of IMVS experiment. Cole-Cole plot of IMVS signals under (b) lower (35 nW) and (c) higher excitation light power (1 mW).

Shunt resistance and the IMVS feature in the low power region

Shunt corresponds to the current loss due to unavoidable imperfection caused by pinholes, morphology, etc. Usually, the shunt process is treated as a resistance that is independent of voltage.[10,11] Therefore if the slower arc obtained in the low power region is determined by the shunt process, we should observe a feature in the IS result in the same frequency range. However, we do not observe any short circuit IS feature corresponding to the slow arc of the IMVS result in the low power region, thus the shunt resistance is not the reason for the IMVS feature in the low power region.

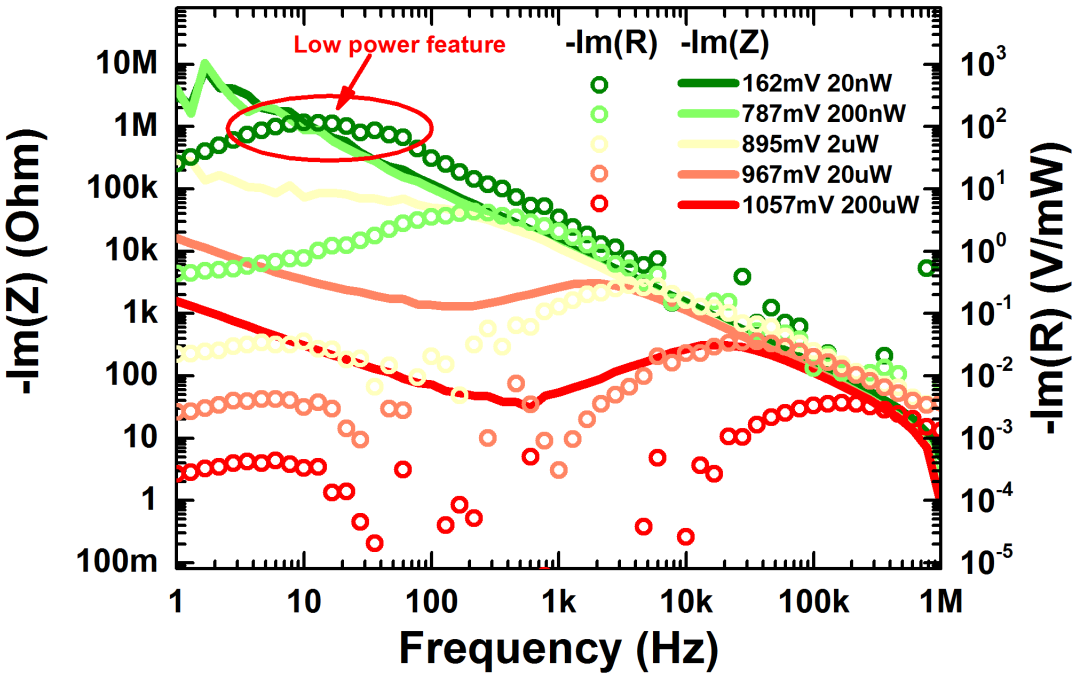

Fig. S3. IMVS (- Im(R)) and IS (- Im(Z)) results obtained under low excitation light intensity. The IS results are measured under short circuit condition.

Math to separate the two relaxation lifetimes.

Although the relaxation time constant is read from the peak in –Im(R), it is not straightforward when multiple peaks coexist. A standard method to extract relaxation time constants more reliably is to fit the IMVS result to the response of an equivalent circuit using both the imaginary and real parts of R. For the case of two time constants, an equivalent circuit shown in the inset of Fig. S4a is convenient[12–16]. Assuming that 100% of the incident photons are converted into current (P(t) => J(t)), the measured result (voltage per unit power) are rescaled to impedance (voltage per unit photocurrent, Ohm). This fitting is used only to separately find out the high frequency component and the low frequency component from the measured result as shown by

the blue and purple circles in Fig. 1c. Refer to Zurazua's work for the physical meaning of the elements in the circuit.[12] The power dependence of the circuit elements are shown in Fig. S4a and the lifetimes of the two component (R_s*C_s and R_b*C_b) are shown in Fig. 1c. The fitted lifetimes (not the circuit elements) using different equivalent circuits do not vary much because the experiment data to be fitted are the same. As an example, circuit elements fitted from another equivalent circuit shown by Fig. S4b inset is shown by Fig. S4b, along with the corresponding lifetimes (R_s*C_s and R_b*C_b) shown in Fig. S5 which is very similar to Fig. 1c.

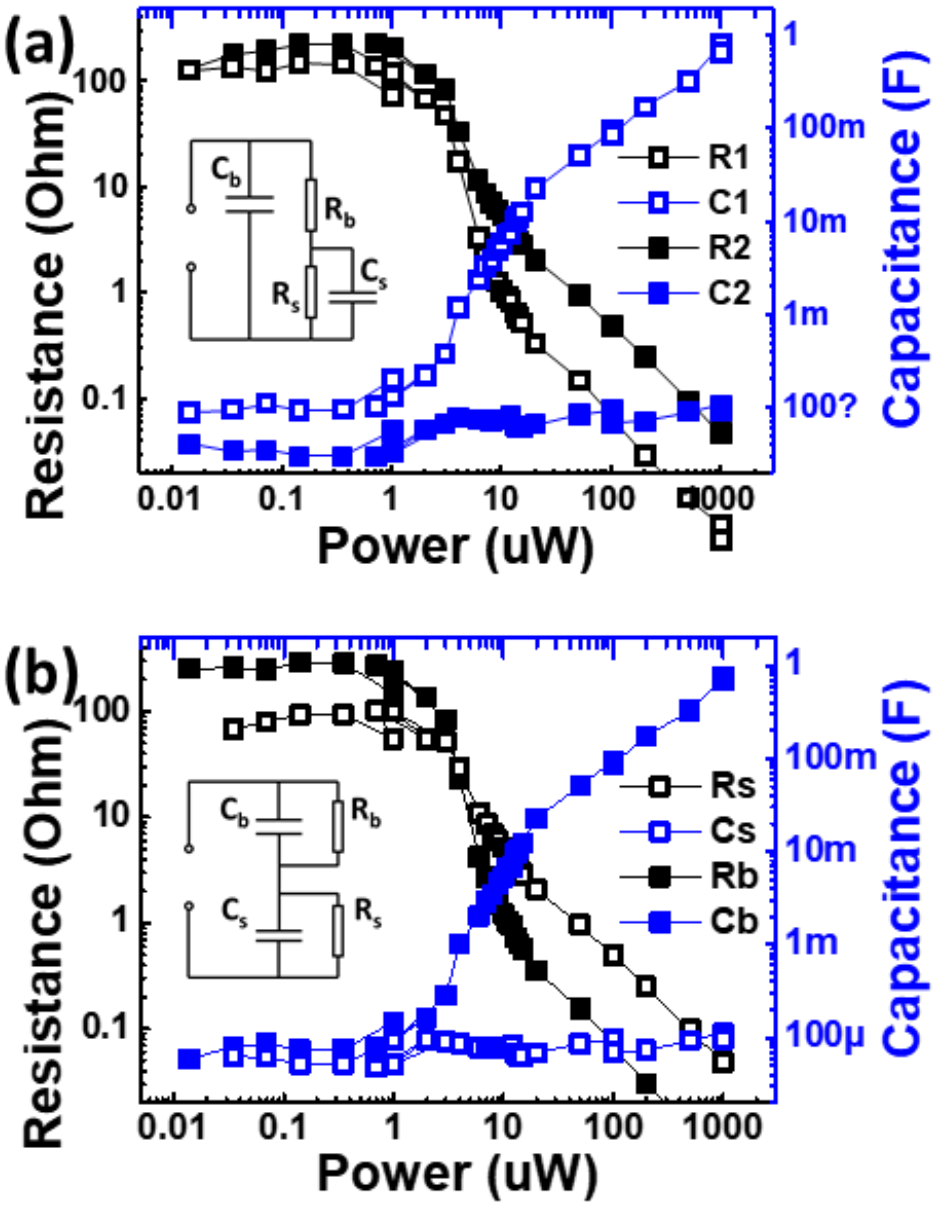

Fig. S4. (a) Fitted circuit element using the equivalent circuit shown by inset. (b) Fitted circuit element using another employed equivalent circuit shown by the inset.

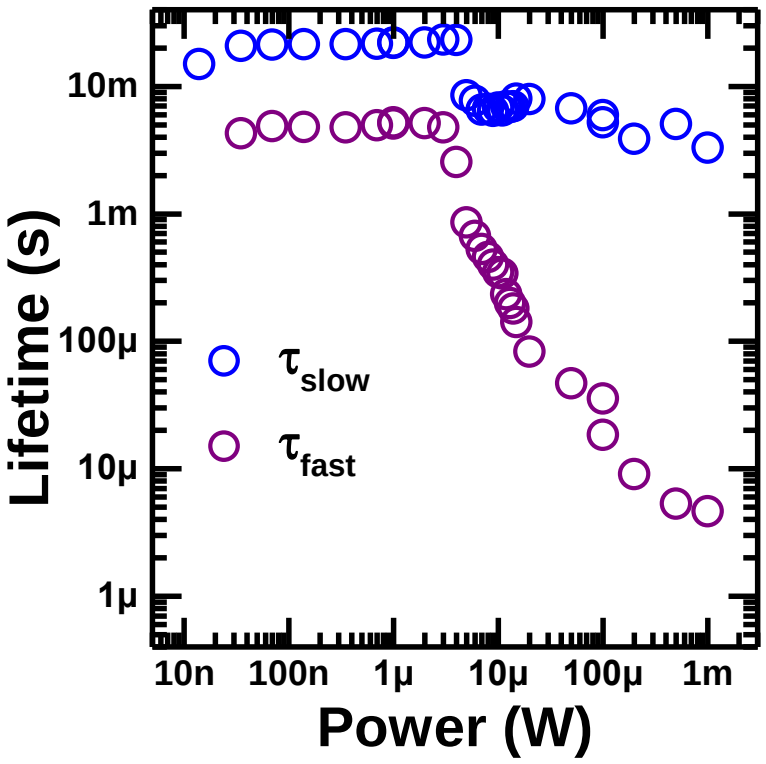

Fig. S5. Decoupled lifetime according to the equivalent circuit shown by inset of Fig. S4b.

Experiment setup of our results in Fig. 4 and 5

Fig. 4 experiment. As shown in Fig. S6, we tried to minimize the illumination reaching to the dark device in the two-device experiment shown in Fig. 4. The whole glass surface of the substrate is covered by a piece of black paper with one small hole (ϕ <1.5 mm). The device under the small hole (right hand side) is illuminated with a carefully focused laser beam. The beam direction is slightly tilted away from the other device (left-hand-side). Two apertures are introduced to constrain the beam direction. This setup minimizes the leaked light scattering to the dark device because the light

propagation inside perovskite layer will be absorbed within 1 μm[17] and the light propagation direction inside glass via reflection is away from the dark device.

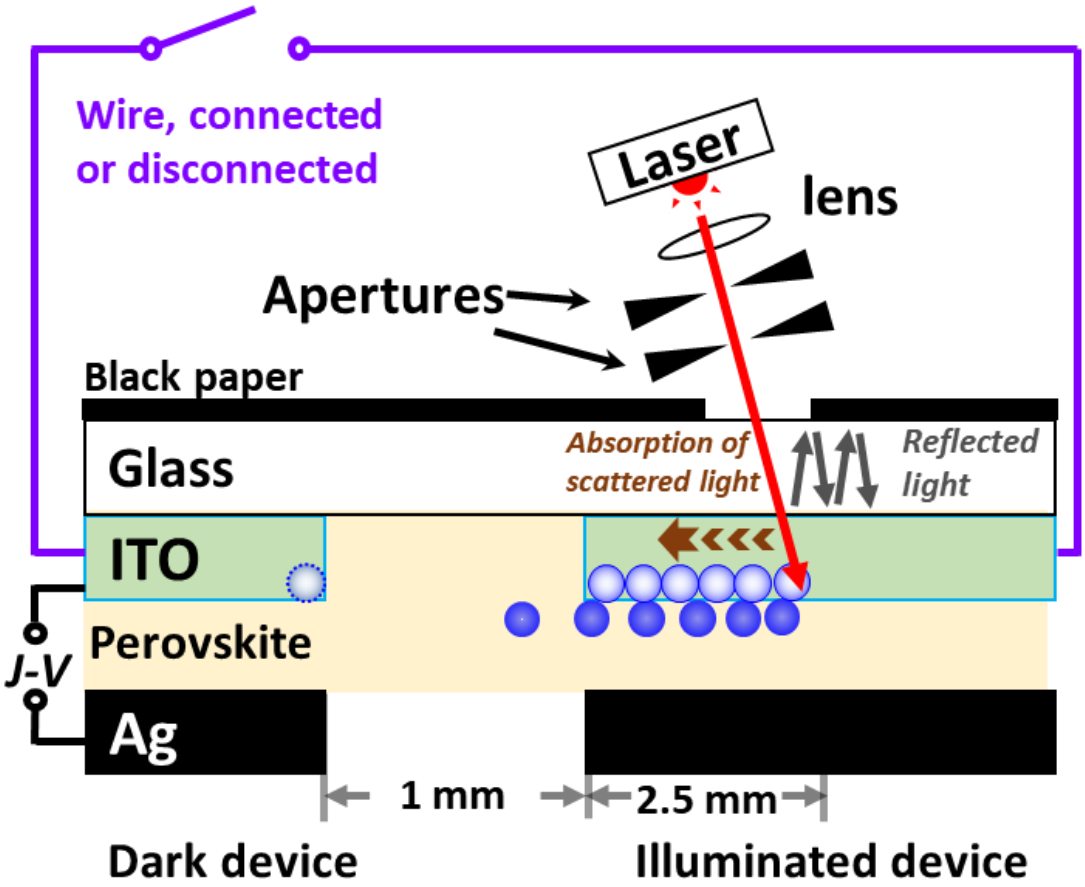

Fig. S6. Setup to minimize the illumination to the dark device in the two-device experiment.

Fig. 5 experiment. The laser was modulated with an NF model WF1974 function generator when the time-dependent device current was monitored with an oscilloscope. In order to measure the low current shown in Figure 5, a current preamplifier (model SR570) was employed.

Sublinear power dependence in presence of only free electrons and holes

General sublinear power dependence

If only the bulk free carriers are involved in the recombination process, the creation and decay of the free carrier is described by,

$$\frac{\mathrm{d}n(\mathrm{or}\ p)}{\mathrm{d}t} = GP - uP^v * n(\mathrm{or}\ p) \qquad \text{(S1)}$$

where n (p) is the free electron (hole) density, G is the quantum yield of the free carrier generation under the photo the power dependence of k on power ($k = uP^v$, where u and v are constant parameters) cannot be linear ($\mathrm{v} = 1$) or superlinear ($\mathrm{v} > 1$). Under quasi-steady condition

We arrive at

$$\mathrm{n(or\ p)} \propto P^{1-v} \qquad \text{(S2)}$$

If $\mathrm{v} \geq 1$, the free carrier density will reduce under higher excitation power, which is not reasonable according to the common understanding. Next, we analyze the power index of recombination rate of a specific mechanisms.

Power dependence of a specific relaxation mechanism

Free carrier dynamics under the photogeneration is described by Eq. S3,

$$\frac{dn(or\ p)}{dt} = GP - k * n(or\ p) \qquad \text{(S3)}$$

where n(or p) is the free electron (or hole) density, t is time, G is the quantum yield of free carriers per unit power, P is the excitation light power, k is the relaxation rate. As

widely reported[18–21], k is found to be dependent on n (or p) determined by the excitation light power. The dependence can be described according to the following Tayler series

$$k = \sum_i k_i n^{i-1}\left(\text{or } p^{i-1}\right) = k_\alpha n^{\alpha-1}(\text{or } p^{\alpha-1}) \qquad \text{(S4)}$$

where $k_i = \frac{1}{(i!)}\frac{d^i k}{dn^i}$ (i = 1, 2, 3…) is the ith order coefficient of the Tayler series.[18] Usually, the first order process is assigned to the monomolecular exciton recombination, or trap-assisted recombination (SRH recombination); the second order process is assigned to the band-to-band recombination (or bimolecular recombination) between bulk free carriers; the third order process is assigned to the Auger recombination.[18–21] In any specific carrier density range, the recombination should be dominated by one specific recombination mechanism, in which case, the right-most expression in Eq. S4 with a specific power index α is appropriate. Under quasi-steady condition ($\frac{dn(or\ p)}{dt} = 0$), we will arrive at $n \propto P^{1/\alpha}$ and the power dependence of k on P is $k \propto P^{1-1/\alpha}$ from Eqs. S3 and S4. With the reasonable assumption that n will increase when the excitation light power increase (namely $\alpha > 0$), the power dependence of k is always sublinear ($(1 - 1/\alpha) < 1$), irrespective of the decay mechanism (Eq. S4). In particular, when the bimolecular recombination (or band-to-band recombination) is dominant, we come to $\alpha = 2$ and $k \propto P^{0.5}$. Such dependence is observed in the organic solar cells and DSSCs[1,22–28]. By contrast in PSCs, it is reported that $k \propto P^1$,[12,29] which is mathematically *impossible* in the

conventional picture involving only free carriers because the power index of $k \propto P^{1-1/\alpha}$ is smaller than 1.

References

1 Y. T. Set, B. Li, F. J. Lim, E. Birgersson and J. Luther, *Appl. Phys. Lett.*, 2015, **107**, 173301.

2 R. Azmi, S. Sinaga, H. Aqoma, G. Seo, T. K. Ahn, M. Park, S.-Y. Ju, J.-W. Lee, T.-W. Kim, S.-H. Oh and S.-Y. Jang, *Nano Energy*, 2017, **39**, 86–94.

3 C. S. Choi, I. K. Moon and N. Kim, *Appl. Phys. Lett.*, 2009, **94**, 60–62.

4 U.-H. Lee, R. Azmi, S. Sinaga, S. Hwang, S. H. Eom, T.-W. Kim, S. C. Yoon, S.-Y. Jang and I. H. JUNG, *ChemSusChem*, 2017, 3780–3787.

5 P. R. F. Barnes, K. Miettunen, X. Li, A. Y. Anderson, T. Bessho, M. Grätzel and B. C. O'Regan, *Adv. Mater.*, 2013, **25**, 1881–1922.

6 S. Wheeler, D. Bryant, J. Troughton, T. Kirchartz, T. M. Watson, J. Nelson and J. R. Durrant, *J. Phys. Chem. C*, 2017, **121**, 13496–13506.

7 D. Kiermasch, P. Rieder, K. Tvingstedt, A. Baumann and V. Dyakonov, *Sci. Rep.*, 2016, **6**, 39333.

8 M. Habibi, F. Zabihi, M. R. Ahmadian-Yazdi and M. Eslamian, *Renew. Sustain. Energy Rev.*, 2016, **62**, 1012–1031.

9 Z. Xiao, Q. Dong, C. Bi, Y. Shao, Y. Yuan and J. Huang, *Adv. Mater.*, 2014, **26**, 6503–6509.

10 D. Bozyigit, W. M. M. Lin, N. Yazdani, O. Yarema and V. Wood, *Nat. Commun.*, 2015, **6**, 6180.

11 B. Qi and J. Wang, *Phys. Chem. Chem. Phys.*, 2013, **15**, 8972–8982.

12 I. Zarazua, G. Han, P. P. Boix, S. Mhaisalkar, F. Fabregat-Santiago, I. Mora-Seró, J. Bisquert and G. Garcia-Belmonte, *J. Phys. Chem. Lett.*, 2016, **7**, 5105–5113.

13 B. C. O'Regan, K. Bakker, J. Kroeze, H. Smit, P. Sommeling and J. R. Durrant, *J. Phys. Chem. B*, 2006, **110**, 17155–17160.

14 A. Guerrero, G. Garcia-Belmonte, I. Mora-Sero, J. Bisquert, Y. S. Kang, T. J. Jacobsson, J. P. Correa-Baena and A. Hagfeldt, *J. Phys. Chem. C*, 2016, **120**, 8023–8032.

15 Y. Shao, Y. Yuan and J. Huang, *Nat. Energy*, 2016, **1**, 15001.

16 M. Bag, L. A. Renna, R. Y. Adhikari, S. Karak, F. Liu, P. M. Lahti, T. P. Russell, M. T. Tuominen and D. Venkataraman, *J. Am. Chem. Soc.*, 2015, **137**, 13130–13137.

17 S. D. Stranks, S. D. Stranks, G. E. Eperon, G. Grancini, C. Menelaou, M. J. P. Alcocer, T. Leijtens, L. M. Herz, A. Petrozza and H. J. Snaith, *Science*, 2014, **342**, 341–344.

18 C. Wehrenfennig, G. E. Eperon, M. B. Johnston, H. J. Snaith and L. M. Herz, *Adv. Mater.*, 2014, **26**, 1584–1589.

19 M. B. Johnston and L. M. Herz, *Acc. Chem. Res.*, 2016, **49**, 146–154.

20 J. W. Jung, C. C. Chueh and A. K. Y. Jen, *Adv. Energy Mater.*, 2015, **5**, 1500486.

21 S. D. Stranks, V. M. Burlakov, T. Leijtens, J. M. Ball, A. Goriely and H. J. Snaith, *Phys. Rev. Appl.*, 2014, **2**, 1–8.

22 J. A. Anta, F. Casanueva, G. Oskam and Ä. De Quı, *J. Phys. Chem. B*, 2006, **110**, 5372–5378.

23 H. J. Snaith, L. Schmidt-Mende, M. Grätzel, M. Chiesa, M. Gr??tzel and M. Chiesa, *Phys. Rev. B*, 2006, **74**, 045306.

24 G. Schlichthörl, S. Y. Huang, J. Sprague and a J. Frank, *J. Phys. Chem. B*, 1997, **101**, 8141–8155.

25 B. C. O'Regan, S. Scully, a C. Mayer, E. Palomares and J. Durrant, *J. Phys. Chem. B*, 2005, **109**, 4616–4623.

26 C. G. Shuttle, B. O'Regan, a. M. Ballantyne, J. Nelson, D. D. C. Bradley, J. De Mello and J. R. Durrant, *Appl. Phys. Lett.*, 2008, **92**, 1–4.

27 R. Hamilton, C. G. Shuttle, B. O'Regan, T. C. Hammant, J. Nelson and J. R. Durrant, *J. Phys. Chem. Lett.*, 2010, **1**, 1432–1436.

28 A. C. Fisher, L. M. Peter, E. A. Ponomarev, A. B. Walker and K. G. U. Wijayantha, *J. Phys. Chem. B*, 2000, **104**, 949–958.

29 A. Pockett, G. Eperon, N. Sakai, H. Snaith, L. M. Peter and P. J. Cameron, *Phys. Chem. Chem. Phys.*, 2017, **19**, 5959–5970.